# Zinc transfer potentials of the $\alpha$- and $\beta$-clusters of metallothionein are affected by domain interactions in the whole molecule

**Li-Juan Jiang*, Milan Vašák†, Bert L. Vallee*, and Wolfgang Maret*‡**

*Center for Biochemical and Biophysical Sciences and Medicine, Harvard Medical School, Seeley G. Mudd Building, 250 Longwood Avenue, Boston, MA 02115; and †Institute of Biochemistry, University of Zurich, Winterthurerstrasse 190, CH-8057 Zurich, Switzerland

Contributed by Bert L. Vallee, December 30, 1999

**The $\alpha$- and $\beta$-polypeptides of human metallothionein (isoform 2), obtained by chemical synthesis, were converted into their respective zinc/thiolate clusters, and each domain was investigated separately. Proton titration data for the N-terminal $\beta$-domain fit a simple model with three ionizations of the same apparent $pK_a$ value of 4.9 and a collective binding constant for zinc of $5 \times 10^{-12}$ M at pH 7.0. The zinc cluster in the C-terminal $\alpha$-domain is more stable than that in the $\beta$-domain. Its pH titration is also more complex, indicating at least two classes of zinc sites with different affinities. The whole molecule is stabilized with regard to the individual domains. Chemical modification implicates lysine side chains in both the stabilization of the $\beta$-domain cluster and the mutual stabilization of the domains in the whole molecule. The two zinc clusters also differ in the reactivity of their cysteine sulfurs and their potential to donate zinc to an acceptor molecule dependent on its type and characteristics. The isolated $\beta$-domain cluster reacts faster with Ellman's reagent and is a better zinc donor toward zinc-depleted sorbitol dehydrogenase than is the isolated $\alpha$-domain cluster, whereas the reverse is observed when a chelating agent is the zinc acceptor. Thus, although each cluster assembles independently of the other, the cumulative properties of the individual domains do not suffice to describe metallothionein either structurally or functionally. The two-domain structure of the whole molecule is important for its interaction with ligands and for control of its reactivity and overall conformation.**

The coordination of zinc in metallothionein (MT) involves a network of interactions with cysteine sulfurs organized into distinct and separate zinc/thiolate clusters in two protein domains, three zinc/nine sulfur atoms (12 zinc/sulfur bonds) in one domain and four zinc/11 sulfur atoms (16 zinc/sulfur bonds) in the other (1, 2). In the N-terminal $\beta$-cluster, each of the three zinc atoms resides in what is essentially the same coordination environment constituted by two terminal and two bridging cysteine ligands. The three bridging sulfurs and their three corresponding zinc atoms are arranged in a chair conformation. In the C-terminal $\alpha$-cluster, the use of five bridging ligands leads to two types of coordination environments: the coordination of two zinc atoms is identical to that of the $\beta$-cluster, whereas the other two each bind three bridging and only one terminal cysteine ligand. The protein envelops the two clusters such that the zinc atoms are completely shielded from solvent while in clefts on each domain three sulfur atoms in particular are exposed to solvent. Owing to the absence of domain interactions detectable by NMR, the orientation of the domains relative to each other in solution is unknown and the domains, therefore, appear as independent units (1). The link between the domains is seen in crystals of MT, however. Hydrogen bonds from lysine-31 in the linker region to the $\beta$-cluster and strengthening of that hydrogen-bonding network by phosphate are thought to stabilize the domains in an overall conformation that has been compared with that of a dumbbell (2, 3).

The number of zinc and sulfur atoms in these clusters seemingly has made it improbable to dissect the chemical and physical characteristics of the whole molecule. Many properties such as the rates of zinc exchange between intact MT molecules (4) are a composite of those of the two clusters. One approach to assigning specific properties to each of the clusters or even to single zinc or sulfur atoms is to use the individual domains of MT, which have been generated by limited proteolysis (5), chemical synthesis (6), and molecular cloning (7). Their characterization essentially has been limited to demonstrating the independent assembly of the clusters in the presence of metal to yield structures that have been assumed to be similar to those encountered in the whole molecule. Functional studies, however, are lacking, because there was no molecular function of MT that had been linked specifically to zinc and that could have been examined. In this regard, we have summarized that the zinc cluster structure of MT is the basis for its functional potential (8) and recently reported properties of MT that are related to its zinc content. In particular, we have demonstrated that the redox-active sulfurs constitute an environment favorable for the redox-inert zinc atoms (9). Consequently, we have studied the properties of MT as a redox-modulated zinc donor/acceptor (10, 11), its interaction with the glutathione redox pair and with ATP (10, 12), and the properties of the apoprotein thionein in displacing zinc from enzymes that are inhibited by tightly bound zinc (13).

In the following study, the individual zinc-reconstituted clusters in the isolated domains are characterized and compared with those in the whole molecule. Both the analytical and synthetic aspects of this approach provide insights. The $\alpha$- and $\beta$-clusters differ significantly in terms of metal binding, zinc transfer, and chemical reactivity. On the other hand, the whole MT molecule has certain properties that are not embodied in its individual domains. These portend to be crucial for the interaction of MT with other molecules and its zinc transfer and redox potentials.

BIOCHEMISTRY

## Materials and Methods

**Materials.** Chemicals and biochemicals used here are essentially those described earlier (10, 12).

**Peptide Synthesis.** Peptides corresponding to the two domains of human MT-2 (residues 1–31 with an acetylated N terminus, "$\beta$-domain," and residues 31–61, "$\alpha$-domain") were obtained by solid-phase synthesis in >90% yield when using *N*-$\alpha$-9-fluorenylmethyloxycarbonyl-*S*-acetoimidomethyl-L-cysteine [Fmoc-Cys(Acm)] as the protected cysteine residue. An ABI 433A solid-phase peptide synthesizer was loaded with Fmoc Lys (Boc)-Wang resin (*p*-benzyloxybenzyl resin; Bachem). All amino acids in the synthesis were *N*-$\alpha$-Fmoc-protected, with the functional groups in the side chain protected as follows: *O*-t-butylaspartic and glutamic acids, *O*-t-butylserine and *O*-t-butylthreonine, lysine (Boc),

Abbreviations: MT, metallothionein; SDH, sorbitol dehydrogenase (EC 1.1.1.14); PAR, 4-(2-pyridylazo)resorcinol; DTNB, 5,5′-dithio-*bis*(2-nitrobenzoic acid); apo-SDH, zinc-depleted SDH.

‡To whom reprint requests should be addressed. E-mail: wolfgang_maret@hms.harvard.edu.

The publication costs of this article were defrayed in part by page charge payment. This article must therefore be hereby marked "*advertisement*" in accordance with 18 U.S.C. §1734 solely to indicate this fact.

and cysteine (Acm) (Bachem). Each protected amino acid was added to the synthesizer in turn, and an Fmoc/*O*-benzotriazol-1-yl-*N,N,N′,N′*-tetramethyluronium hexafluorophosphate (HBTU) monitor was used to follow the incorporation into the peptide. On completion of the synthesis, the peptide was cleaved and non-Acm protecting groups were removed by using a solution of 0.75 g of phenol, 0.25 ml of ethanedithiol, 0.5 ml of thioanisole, 0.5 ml of water, and 10 ml of trifluoroacetic acid. The peptide then was precipitated with t-butyl methylether and purified by gel filtration on Sephadex G-25 in 0.1% trifluoroacetic acid. The Acm group was removed by dissolving the peptide in acetic acid containing silver nitrate, stirring at 0°C for 1 h, followed by precipitation of the peptide with ether, isolation by centrifugation, and treatment with DTT in acetic acid at 25°C for 3 h. The purity of the peptides as determined by HPLC was higher than 93%. The correctness of the synthesis was verified by electrospray MS.

**Preparation of Zinc- and Cadmium-Reconstituted $\alpha$- and $\beta$-Clusters of Human MT-2.** Lyophilized synthetic $\alpha$- (or $\beta$-) domain (2 mg) was incubated with 20 mg of DTT in 20 mM Tris·HCl, pH 8.6, overnight at room temperature (14). The sample then was titrated to pH 1 with HCl and applied to a Sephadex G-10 column ($1 \times 100$ cm) that was preequilibrated with 10 mM HCl at room temperature. The protein was eluted with 10 mM HCl at a flow rate of 8 ml/h. The apoprotein-containing fractions were detected spectrophotometrically (220 nm) and pooled. Five (or four) equivalents of zinc chloride were added to reconstitute the $\alpha$- (or $\beta$-) cluster under a nitrogen atmosphere at 4°C. The reaction mixture was adjusted to pH 8.6 with 1 M Tris base, which was added in small aliquots over a period of 30 min under nitrogen and with stirring. The sample was lyophilized and then taken up in a small volume of 10 mM Tris·HCl, pH 8.6, and excess zinc was removed by a second gel filtration step using the same column and elution procedure with this buffer. The zinc-reconstituted clusters then were lyophilized and stored at 4°C.

The following analytical data are the average from two preparations. Quantitative amino acid analysis of the zinc-reconstituted clusters is consistent with the theoretical composition and was used to determine the concentrations of the peptides. Accordingly, the $\alpha$-cluster contained $3.9 \pm 0.1$ zinc atoms per molecule and $10.7 \pm 0.3$ sulfhydryls were titrated with 2,2′-dithiodipyridine, whereas the $\beta$-cluster contained $3.0 \pm 0.1$ zinc atoms and $8.6 \pm 0.2$ sulfhydryls were titrated. Of the total zinc found in the $\alpha$- and $\beta$-clusters, only 2.5% and 5.3%, respectively, were chelatable with 125 $\mu$M zincon (2′-hydroxyl-5′-sulfoformazylbenzene).

Cadmium-containing clusters were prepared and characterized in an analogous manner.

**pH Titrations of the Domain Peptides.** The absorbances at 220 and 250 nm have been used to determine zinc and cadmium dissociation, respectively, from the clusters as a function of pH (15). The $\alpha$- and $\beta$-clusters were dissolved in 1 ml of 100 mM sodium perchlorate and the pH was changed with 5–500 mM perchloric acid and measured with a micro-NMR pH electrode (Orion, Boston) at 25°C.

**Kinetic Studies of the Reaction Between Domain Peptides and 5,5′-Dithiobis(2-Nitrobenzoic Acid) (DTNB).** The thiol reactivity of the clusters was assayed spectrophotometrically at 412 nm and 25°C with Ellman's reagent (DTNB) under two different pseudo-first-order rate conditions in which either [DTNB] $\ll$ [cluster thiols] (12, 16) or [DTNB] $\gg$ [cluster thiols] (17). In the first instance, the reactivity of the clusters (10 $\mu$M) with DTNB (4 $\mu$M) was measured in 0.2 M Tris·HCl, pH 7.4 (12), whereas in the second instance, clusters (5 $\mu$M) and DTNB (from 0.25 to 1.5 mM) were reacted in 5 mM Tris·HCl, pH 7.4, containing 0.1 M KCl (17). All data were analyzed as first-order reactions by plotting $\ln(A_\infty - A_t)$ vs. time.

**Kinetic Studies of the Reaction Between Domain Peptides and 4-(2-Pyridylazo)Resorcinol (PAR).** PAR (200 $\mu$M) was incubated with clusters (2 $\mu$M) in 0.2 M Tris·HCl, pH 7.4, and the formation of the $Zn(PAR)_2$ complex followed at 500 nm (18). Kinetics were analyzed by using semilog plots of $(A_\infty - A_t)/(A_\infty - A_0)$, where $A_t$ is the observed absorbance at time $t$, $A_0$ is the absorbance at $t = 0$, and $A_\infty$ is the absorbance at completion of the reaction as evaluated with the method of Guggenheim (19).

**Lysine Modification.** Lysines of MT and of the domain peptides were modified by carbamoylation with potassium cyanate (20). Excess reagent and buffer were removed by passing the proteins through a PD-10 column (Amersham Pharmacia) that had been equilibrated with water. Protein concentrations were determined by titration of sulfhydryls with 2,2′-dithiodipyridine.

**Reconstitution of Zinc-Depleted Sorbitol Dehydrogenase (Apo-SDH) by the Domain Clusters.** The $\alpha$- or $\beta$-clusters were incubated with 1.7 $\mu$M apo-SDH in 0.2 M Tris·HCl, pH 7.4, at $22.5 \pm 0.5$°C. Aliquots were withdrawn periodically and assayed for enzymatic activity (10).

## Results

**Spectral Properties of the Domain Peptides.** Based on the protein concentration as determined by amino acid analysis, the molar extinction coefficients (220 nm) of the $\alpha$- and $\beta$-apoforms at pH 2 are 22,100 and 19,200 $M^{-1}\cdot cm^{-1}$, respectively, whereas those of the zinc-reconstituted $\alpha$- and $\beta$-clusters at pH 7.4 are 78,900 and 69,100 $M^{-1}\cdot cm^{-1}$, respectively. The extinction coefficients (220 nm) of native human apo- and holo-MT at these pH values, i.e., 48,000 and 159,000 $M^{-1}\cdot cm^{-1}$ (21), exceed the sum of the extinction coefficients for each domain.

The analytical data, i.e., zinc and sulfhydryl content of the clusters (see *Materials and Methods*), the characteristics of their absorption and CD spectra (not shown), and the fact that zinc is tightly bound all indicate that each apopeptide interacts with zinc to form a cluster in the absence of the other domain. Preliminary studies by two-dimensional NMR show the polypeptide fold around the zinc and cadmium $\alpha$-cluster to be virtually identical to that in the whole molecule. However, the position of the resonance of cadmium atom designated number 6 in the NMR spectra of the $\alpha$-cluster is shifted slightly downfield from that in the whole molecule (22), indicating subtle changes in coordination of this metal site in the cluster. Owing to the increased flexibility of the isolated $\beta$-domain, a high-resolution NMR structure of the latter has not been obtained.

**pH Titrations of the Domain Peptides and the Whole Molecule.** The chromophoric properties of the metal–thiolate complexes of MT provide a means to assess the stability of the metal–protein complex by pH titrations. Displacement of zinc by protons results in a decrease of absorbance at 220 nm, reflecting a charge-transfer transition of the Zn—S (Cys) bond (15). The absorbance remains virtually constant above pH 7, but decreases sharply in a narrow range between pH 4 and 5.8 (Fig. 1*A*). The point of half-maximum absorbance for the $\alpha$-cluster is 0.3 pH unit lower than that for the $\beta$-cluster, which titrates with an apparent $pK_a$ of 4.9, demonstrating that zinc binds more tightly to the $\alpha$-cluster. To exclude that changes in peptide conformation as a function of pH affect these absorbance changes at 220 nm, titrations of the individual cadmium-reconstituted domains were monitored at both 220 and 250 nm. In contrast to zinc, the charge-transfer transition of the Cd—S (Cys) bond at 250 nm is well separated from the absorbance of the peptide backbone at 220 nm. Thus, the titration data for the cadmium peptides confirm the additional stabilization of the cluster in the $\alpha$-domain with regard to that in the $\beta$-domain (Fig. 1*B*). The stabilization by 0.5 pH unit is slightly more than that for the zinc peptides (0.3 pH unit, see above). Based on the assumption that each Zn—S bond contributes equally to the molar absorbance, data

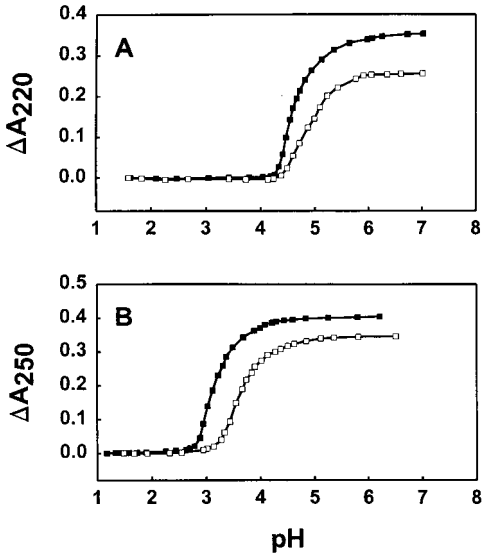


**Fig. 1.** Titrations of zinc-reconstituted (*A*) and cadmium-reconstituted (*B*) $\alpha$-domain (■) and $\beta$-domain (□) vs. pH. The absorbance change at 220 (or 250 nm) was obtained by subtracting the absorbance of the apoproteins at pH $< 2$ from those of the zinc or cadmium proteins at different pH values. Measurements were made on solutions containing 7 $\mu$M clusters and 0.1 M sodium perchlorate. The pH was adjusted with 5–500 mM perchloric acid.

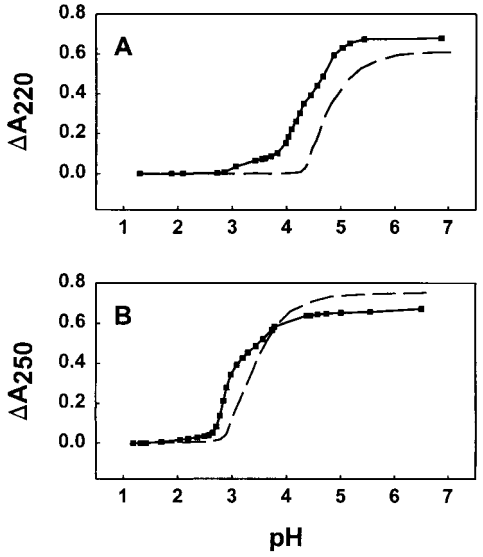


**Fig. 3.** Comparison between the titrations of the whole human zinc (*A*) and cadmium (*B*) MT-2 molecules (■) and the added titrations of their clusters (dashed line). The titrations were performed on MT samples (7 $\mu$M) in 0.1 M sodium perchlorate. The prepeak in zinc MT is caused, in part, by the presence of 0.5 g-atom cadmium in the sample, as has been reported by others (15).

were fitted by a simple model (23). A plot of $\log[\text{M-S}]/[\text{M}][\text{H}_n\text{S}]$ vs. pH yields a straight line for the $\beta$-cluster, indicating the independent binding of three zinc ions with an average apparent $K_D$ value of $5 \times 10^{-12}$ M at pH 7 (Fig. 2*A*). According to the value of $n = 3$ obtained from the slope, three protons are required to displace one zinc atom from its binding site, commensurate with the loss of absorption over such a narrow pH interval and consistent with liberation of an average of three protons upon the addition of one equivalent of Cd(II) to apo-MT (24). An analogous plot yields an apparent $K_D$ value of $5.8 \times 10^{-16}$ M for dissociation of cadmium from the $\beta$-domain. The data for the $\alpha$-cluster yield a nonlinear plot (Fig. 2*B*) and reveal at least two classes of zinc sites with different

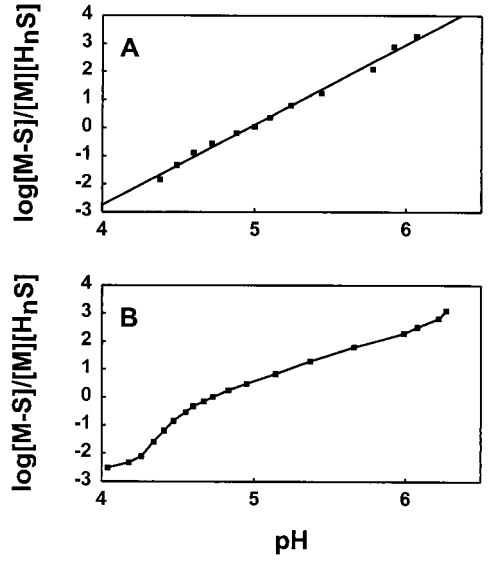


**Fig. 2.** Replots of the data for zinc-reconstituted $\beta$-domain (*A*) and $\alpha$-domain (*B*) from Fig. 1 (23).

binding constants and cooperativity with regard to protons, with $n > 3$ at low pH and $n = 2$ at high pH.

Human $Zn_7$-MT-2 titrates with an apparent $pK_a$ value of 4.3, compared with 4.4 for equine $Zn_7$-MT (15). A comparison between the titration of human $Zn_7$-MT-2 and the sum of the titrations of its domains demonstrates a stabilization of the intact molecule by 0.5 pH unit (Fig. 3*A*). Similarly, a difference of 0.4 pH unit is observed between cadmium MT-2 and the sum of its individual domains (Fig. 3*B*). These observations suggest interactions in the whole molecule that are not revealed in studies of the individual domains. The only interaction is known from crystallographic studies of MT; it is a hydrogen bond from Lys-31 in the linker region to the sulfur atom of Cys-19 and to the backbone carbonyls of Cys-19 and Cys-21 in the $\beta$-domain (2). Lys-31 is also the binding site for phosphate that bridges the domains and has been deemed critical for the crystallization of MT (3). Therefore, it was tested whether or not these interactions in the whole molecule involve lysine side chains. With regard to the unmodified zinc $\alpha$-domain, the lysine-modified $\alpha$-domain is stabilized (Fig. 4*A*). In contrast, the zinc $\beta$-domain is destabilized when its lysines are modified and zinc binding is less cooperative with regard to protons (Fig. 4*B*). Lysine-modified MT also is destabilized relative to MT (Fig. 4*C*). The apparent $pK_a$ value of lysine-modified MT is identical with that of the sum of the two modified individual domains (Fig. 4*C*). Thus, the additional stabilization of the whole molecule is lost by lysine carbamoylation, attesting to the critical role of the evolutionarily conserved lysines in MT.

**Comparison of the Sulfhydryl Reactivity of the Zinc Clusters.** Under pseudo-first-order rate conditions when the concentration of DTNB is less than one equivalent per sulfur ([DTNB] $\ll$ [cluster thiols]), the $\beta$-cluster reacts faster than the $\alpha$-cluster (Fig. 5). The rate constants for the initial process are $4.9 \times 10^{-3}$ s$^{-1}$ for the $\alpha$-cluster and $1.4 \times 10^{-2}$ s$^{-1}$ for the $\beta$-cluster (Fig. 5 *Inset*). The rate constant for human $Zn_7$-MT-2 ($2.8 \times 10^{-3}$ s$^{-1}$) (12) is very similar to that of the $\alpha$-cluster.

Under conditions when [DTNB] $\gg$ [cluster thiols] in the range from 15 to 100, the kinetics of both clusters are biphasic. The observed rate constants are clearly DTNB dependent. Plots of the

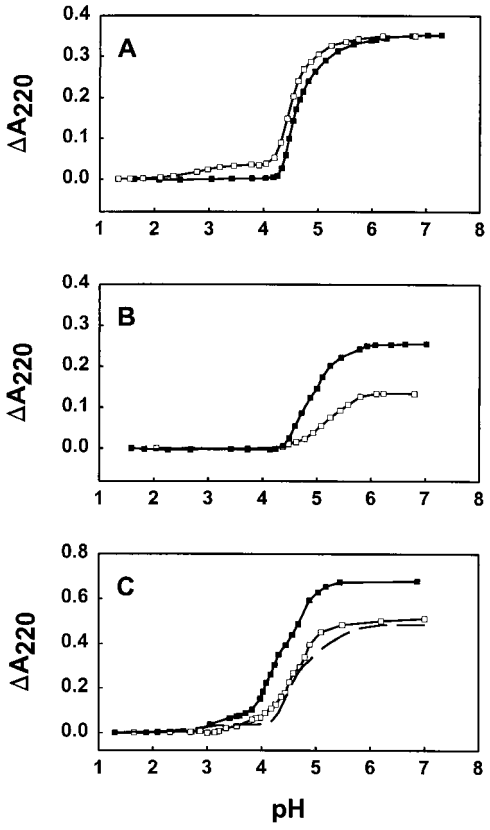


**Fig. 4.** Proton titrations of unmodified (■) and Lys-carbamoylated (□) α-domain (*A*), β-domain (*B*), and zinc MT-2 (*C*). Added titrations of the lysine-modified domains (dashed line) are shown. The data for the unmodified proteins are from Figs. 1 and 3.

observed rate constant of the fast step vs. the concentration of DTNB are linear with a finite intercept (Fig. 6*A*), indicating both DTNB-dependent and DTNB-independent components with a rate law $v = k_1 + k_2$[DTNB] (17). The first-order constants for the DTNB-independent processes (intercept) are $k_{1\alpha} = 0.5 \times 10^{-3}\ s^{-1}$ and $k_{1\beta} = 2.7 \times 10^{-3}\ s^{-1}$, whereas the second-order rate constants for the DTNB-dependent processes (slopes) are $k_{2\alpha} = 1.9\ s^{-1}{\cdot}M^{-1}$ and $k_{2\beta} = 6.1\ s^{-1}{\cdot}M^{-1}$. The reported values for the α-cluster with cadmium are $k_1 = 6.4 \times 10^{-4}\ s^{-1}$ and $k_2 = 1.1\ s^{-1}{\cdot}M^{-1}$ (17), demonstrating that the influence of the metal on the reactivity of MT with DTNB is negligible. The relationship between DTNB and the observed rate constants in the slow step is nonlinear (Fig. 6*B*).

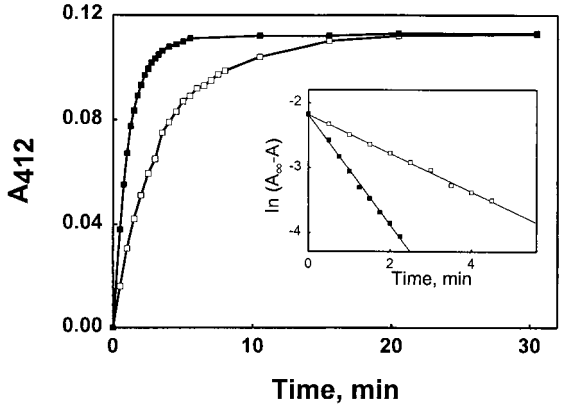


**Fig. 5.** Thiol reactivity of the clusters. Clusters (10 μM) were incubated with DTNB (4 μM) in 0.2 M Tris·HCl, pH 7.4, and 25°C, and the reactions were followed spectrophotometrically (412 nm). (*Inset*) First-order replot of the data. □, α-Domain; ■, β-domain.

**Zinc Transfer from the Clusters to PAR.** When PAR is the zinc acceptor, the amount of zinc released after 1 h from the α-cluster is 2.5-fold higher than that from the β-cluster (Fig. 7). The kinetics of the two reactions are biphasic. Rate constants for the fast and slow steps are $8.4 \times 10^{-4}$ and $9.9 \times 10^{-5}\ s^{-1}$ for the α-cluster and $3.5 \times 10^{-4}$ and $4.3 \times 10^{-5}\ s^{-1}$ for the β-cluster, respectively. The kinetics of zinc transfer from native human MT-2 to PAR (10) are similar to those from the β-cluster, suggesting that initially zinc is released from the β-cluster of MT-2.

**Zinc Transfer from the Clusters to Apo-SDH.** Although MT contains seven zinc atoms, only one of them appears to be available for transfer to apo-SDH (10). The reconstitution of apo-SDH by the two clusters was investigated to determine which of them provides the zinc. Exactly one of the three zinc atoms from the β-cluster is transferred to apo-SDH just as observed with the parent protein (Fig. 8*A*), whereas less than one zinc atom is transferred to apo-SDH from the α-cluster (Fig. 8*B*).

Reconstitution of apo-SDH with the clusters is a relatively slow process (Fig. 9), similar to that with the whole MT-2 molecule. The second-order rate constants of these biphasic processes are 37 and $9\ s^{-1}{\cdot}M^{-1}$ for the α-cluster and 357 and $90\ s^{-1}{\cdot}M^{-1}$ for the β-cluster. In comparison, the second-order rate constant for the monophasic reaction of MT-2 is $24\ s^{-1}{\cdot}\ M^{-1}$ (10). Unlike what was observed with PAR, the release of zinc from the β-cluster and its transfer to apo-SDH is almost 10 times faster than that from the α-cluster, suggesting different mechanisms of zinc transfer to these two acceptors.

## Discussion

Although each of the two clusters of MT assembles with zinc cooperatively and independently of the other domain, their properties do not add up to those of the whole molecule. These additional features as a result of the two-domain structure of MT appear to have important implications for the modulation of its zinc transfer potential, the binding of ligands, and, possibly, for the translocation of MT to different compartments in the cell.

**Cluster Structure and Stability.** In conventional metalloproteins the formation of the site destined to coordinate precedes the interaction with the metal, whereas in MT the metal atoms organize the folding of the protein around them. Binding of 7 zinc atoms to 20 evolutionarily conserved cysteine residues results in zinc/sulfur networks, whose ligands are patterned in a manner that the primary sequence of MT would not predict. Owing to the constituent number of zinc and sulfur atoms involved in the formation of the clusters, the physicochemical properties such as zinc-binding constants are averages (15). Individual domain peptides provide the opportunity to determine the properties of each cluster and, ultimately, to determine the contribution of each zinc and sulfur atom. Thus, proton titrations prove the α-cluster to be more stable thermodynamically than the β-cluster (Fig. 1). The $K_D$ value ($5 \times 10^{-12}$ M) for the three zinc atoms in the β-cluster is slightly lower than that of the whole molecule ($1.4 \times 10^{-13}$ M) (25), indicating an additional stabilization in the latter (see below). Each zinc atom is coordinated tetrahedrally with four sulfur ligands (1, 2). Yet, the α-cluster differs from the β-cluster in the manner in which bridging cysteine ligands are deployed. Thus, three bridging and one terminal ligand constitute the coordination environment of two of the four zincs in the α-domain whereas that of all others, including those in the β-domain, is formed by two terminal and two bridging ligands. Two types of zinc coordination environments are apparent

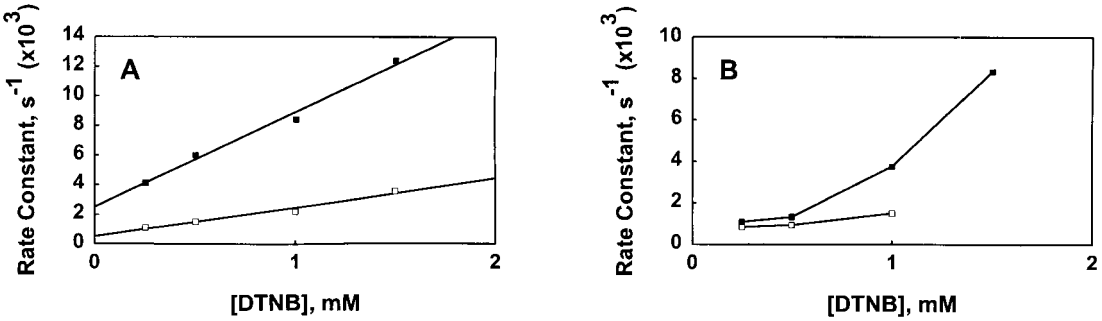


**Fig. 6.** (*A*) Rate constants for the fast step of the reactions between clusters and DTNB as a function of the concentration of DTNB. The reaction of the clusters (5 $\mu$M) and DTNB (from 0.25 to 1.5 mM) was studied in 5 mM Tris·HCl, pH 7.4, containing 0.1 M potassium chloride (17). The data were analyzed as first-order reactions by plotting $\ln[(A_\infty - A_t)/(A_\infty - A_0)]$ vs. time. (*B*) Rate constants for the slow step of the reactions between clusters and DTNB as a function of the concentration of DTNB. □, $\alpha$-Domain; ■, $\beta$-domain.

from the pH titration data of the $\alpha$-cluster, which also suggest that zinc atoms are bound with different affinities (Fig. 2*B*). Accordingly, one possible interpretation for the different cooperativity of proton binding with regard to zinc dissociation in the two domains relates to the different number of bridging atoms. In the $\beta$-domain, the ligand-to-metal ratio is higher than that in the $\alpha$-domain (3.00 vs. 2.75). Yet, this factor does not seem to determine thermodynamic stability. Despite the same number of zinc/sulfur bonds per metal in each domain, the higher connectivity (increasing number of bridges) seems to be the key factor for the higher stability of the $\alpha$-cluster.

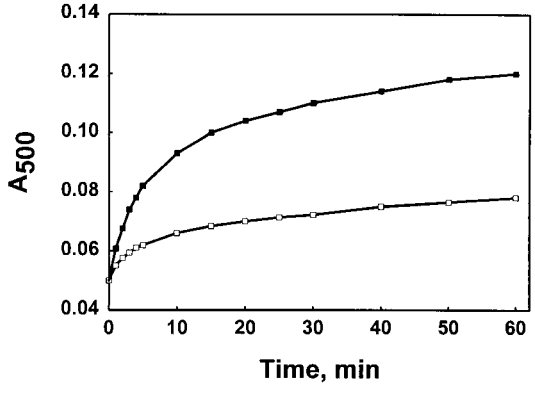


**Fig. 7.** Zinc transfer from clusters to PAR. Clusters (2 $\mu$M) were incubated with PAR (200 $\mu$M) in 0.2 M Tris·HCl, pH 7.4, and the reactions were followed spectrophotometrically (500 nm). ■, $\alpha$-Domain; □, $\beta$-domain.

**Cluster Function and Reactivity.** Our studies have focused on a function of the clusters as redox units in the mobilization and binding of zinc (9) and the modulation of zinc transfer by ligands of MT such as glutathione and ATP (10, 12). Indeed, we have established that the zinc/sulfur bonds of MT react with biological disulfides (26) and selenium compounds (27) and have suggested that the function of MT in zinc metabolism correlates with the redox state of the cell. Hence, we have investigated both the reactivity of the clusters with a disulfide (DTNB) and their roles in zinc transfer.

The reaction of each zinc cluster with excess DTNB is biphasic, which contrasts with an earlier report of a monophasic reaction between the cadmium $\alpha$-cluster and DTNB (17). The difference observed could be caused by the different ranges of DTNB concentrations used in these studies, because we also observe a monophasic process for the $\alpha$-cluster at a concentration of 1.5 mM DTNB. It was concluded previously that the fast step of the reaction of intact MT reflects the higher reactivity of the $\alpha$-cluster and, hence, that the $\alpha$-cluster is more labile kinetically than the $\beta$-cluster (17, 28). Our results would seem to lead to the opposite conclusion: the $\beta$-cluster reacts faster with DTNB than the $\alpha$-cluster.

A description of the structure of the clusters is incomplete without reference to their dynamic behavior. The three metal positions in the $\beta$-domain exchange much faster than those in the four positions of the $\alpha$-domain (29, 30). The clustering of positive

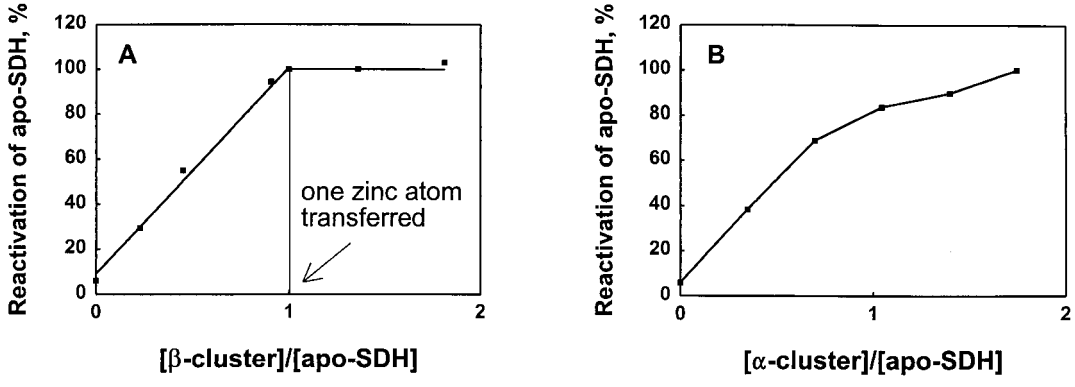


**Fig. 8.** Reconstitution of apo-SDH with the clusters. The $\beta$-domain (*A*) and $\alpha$-domain (*B*) were incubated with apo-SDH (1.7 $\mu$M) in 0.2 M Tris·HCl, pH 7.4, for 1 h at different ratios between zinc and apo-SDH. After equilibration, aliquots were withdrawn from the mixtures and assayed for SDH activity.

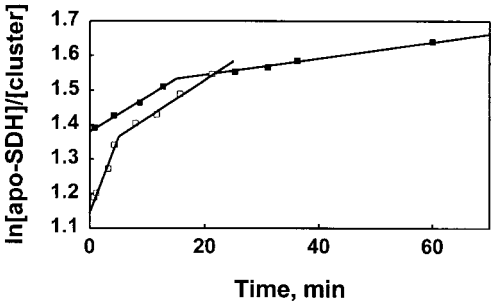


**Fig. 9.** Kinetics of the reconstitution of apo-SDH with the $\alpha$-domain (■) and $\beta$-domain (□). Clusters were incubated with apo-SDH (1.7 $\mu$M) at a molar ratio between zinc in the clusters and apo-SDH of 1.4 in 0.2 M Tris·HCl, pH 7.4. Aliquots (10 $\mu$l) were periodically withdrawn from the mixtures and assayed for SDH activity.

charges from lysine side chains and twice as many NH—S hydrogen bonds as in the $\alpha$-domain have been proposed to stabilize the unliganded sulfhydryls of cysteines in the $\beta$-domain (2). Increased availability of unliganded sulfhydryls would render the $\beta$-domain more reactive toward electrophiles than the $\alpha$-domain, as, for example, supported by its higher reactivity toward iodoacetamide (31).

The potential of the $\alpha$- and $\beta$-clusters to release zinc also differs, but this potential depends on the zinc acceptor. PAR is a small molecule that may attack the metals in the $\alpha$-cluster directly as has been reported for EDTA and nitrilotriacetate (32, 33). This is particularly noteworthy because the thermodynamically less stable $\beta$-cluster is the one that is more stable toward chelating agents. The reason for this may lie in the larger surface accessibility of the sulfur ligands in the $\alpha$-domain (2). In contrast, SDH is a large protein, the active site of which is buried such that it would seem virtually impossible to gain direct access to the metals in the clusters. In that instance, transfer of zinc from the clusters to SDH is thought to occur through a dissociative mechanism. Hence, the reactivity of each cluster would be controlled by specific steric and electronic factors that would depend on the types of reactants.

**Domain Interactions.** The structure and function of the metal ions in the two individual domains of MT are markedly different. Moreover, mutual interactions between the domains affect zinc binding in the clusters in such a way that the properties of the whole molecule are not equal to the sum of its parts. NMR techniques have not detected domain interactions in solutions of MT. Yet, a comparison between the properties of MT-3 and those of its individual clusters (34, 35) revealed that they mutually stabilize each other (36). In accord with these studies, either $^{113}$Cd or $^{1}$H NMR lines of the isolated $\beta$-domain of MT-2 are broad. Because sharp lines are readily recorded in the whole MT molecule and in the isolated $\alpha$-domain, the latter seems to decrease the flexibility of the $\beta$-domain in MT. Also, the presence of the $\beta$-domain is not inconsequential for the structure of the $\alpha$-domain, because, in comparison with MT, a small chemical shift of one of the four $^{113}$Cd resonances in the $\alpha$-domain is observed. Mutual interactions of the domains also were inferred for mouse MT on the basis of nonadditivity of the CD spectra of its domains to yield the spectrum of the whole molecule (37). It appears that in MT the covalent linkage between the $\alpha$- and $\beta$-domains reduces the flexibility of the N and C termini dramatically. At present, a hydrogen bond involving Lys-31 and its interaction with phosphate are the only structural details known that could stabilize the $\beta$-domain in MT crystals. Our chemical modification data suggest that lysines are also important for stabilizing the structure of the $\beta$-domain in solution.

In terms of zinc transfer and thiol reactivity with disulfides, the whole MT molecule is less reactive than its individual clusters, demonstrating that domain interactions in the whole molecule affect its reactivity and structure. Thus, the reactivity of MT is not simply approximated by the sum of the reactivities of its individual domains as has been suggested recently (28). The two-domain structure of MT critically affects the function of each cluster and appears to be crucial for the interaction of that molecule with other ligands such as ATP and associated conformational changes (12) that may control the cellular localization and translocation of MT.

We thank Dr. S. Klauser (University of Zurich) for the synthesis of the peptides. M.V.'s work was supported in part by Swiss National Science Foundation Grant 32-49460.96. This work was supported by the Endowment for Research in Human Biology, Inc.

1. Arseniev, A., Schultze, P., Wörgötter, E., Braun, W., Wagner, G., Vašák, M., Kägi, J. H. R. & Wüthrich, K. (1988) *J. Mol. Biol.* **201,** 637–657.
2. Robbins, A. H., McRee, D. E., Williamson, M., Collett, S. A., Xuong, N. H., Furey, W. F., Wang, B. C. & Stout, C. D. (1991) *J. Mol. Biol.* **221,** 1269–1293.
3. Robbins, A. H. & Stout, C. D. (1991) *Methods Enzymol.* **205,** 485–502.
4. Maret, W., Larsen, K. S. & Vallee, B. L. (1997) *Proc. Natl. Acad. Sci. USA* **94,** 2233–2237.
5. Winge, D. R. & Miklossy, K.-A. (1982) *J. Biol. Chem.* **257,** 3471–3476.
6. Kull, F. J., Reed, M. F., Elgren, T. E., Giardelli, T. L. & Wilcox, D. E. (1990) *J. Am. Chem. Soc.* **112,** 2291–2298.
7. Kurasaki, M., Emoto, T., Arias, A. R. L., Okabe, M., Yamasaki, F., Oikawa, S. & Kojima, Y. (1996) *Protein Eng.* **9,** 1173–1180.
8. Vallee, B. L. (1995) *Neurochem. Int.* **27,** 23–33.
9. Maret, W. & Vallee, B. L. (1998) *Proc. Natl. Acad. Sci. USA* **95,** 3478–3482.
10. Jiang, L. J., Maret, W. & Vallee, B. L. (1998) *Proc. Natl. Acad. Sci. USA* **95,** 3483–3488.
11. Jacob, C., Maret, W. & Vallee, B. L. (1998) *Proc. Natl. Acad. Sci. USA* **95,** 3489–3494.
12. Jiang, L. J., Maret, W. & Vallee, B. L. (1998) *Proc. Natl. Acad. Sci. USA* **95,** 9146–9149.
13. Maret W., Jacob, C., Vallee, B. L. & Fischer, E. H. (1999) *Proc. Natl. Acad. Sci. USA* **96,** 1936–1940.
14. Vašák, M. (1991) *Methods Enzymol.* **205,** 44–46.
15. Vašák, M. & Kägi, J. H. R. (1983) *Metal Ions Biol. Syst.* **15,** 213–273.
16. Cismowski, M. J. & Huang, P. C. (1991) *Biochemistry* **30,** 6626–6632.
17. Savas, M. M., Petering, D. H. & Shaw, C. F., III (1991) *Inorg. Chem.* **30,** 581–583.
18. Shaw, C. F., III, Laib, J. E., Savas, M. M. & Petering, D. H. (1990) *Inorg. Chem.* **29,** 403–408.
19. Guggenheim, E. A. (1926) *Phil. Mag.* **2,** 538–543.
20. Zeng, J. (1991) *Methods Enzymol.* **205,** 433–437.
21. Schäffer, A. (1991) *Methods Enzymol.* **205,** 529–540.
22. Messerle, B. A., Schäffer, A., Vašák, M., Kägi, J. H. R. & Wüthrich, K. (1990) *J. Mol. Biol.* **214,** 765–779.
23. Petering, D. H. & Shaw, C. F., III (1991) *Methods Enzymol.* **205,** 475–484.
24. Kägi, J. H. R. & Vallee, B. L. (1961) *J. Biol. Chem.* **236,** 2435–2442.
25. Kägi, J. H. R. (1993) in *Metallothionein III*, eds. Suzuki, K. T., Imura, N. & Kimura, M. (Birkhäuser, Basel), pp. 29–55.
26. Maret, W. (1994) *Proc. Natl. Acad. Sci. USA* **91,** 237–241.
27. Jacob, C., Maret, W. & Vallee, B. L. (1999) *Proc. Natl. Acad. Sci. USA* **96,** 1910–1914.
28. Munoz, A., Petering, D. H. & Shaw, C. F., III (1999) *Inorg. Chem.* **38,** 5655–5659.
29. Otvos, J. D., Liu, X., Li, H., Shen, G. & Basti, M. (1993) in *Metallothionein III*, eds. Suzuki, K. T., Imura, N. & Kimura, M. (Birkhäuser, Basel), pp. 57–74.
30. Nettesheim, D. G., Engeseth, H. R. & Otvos, J. D. (1985) *Biochemistry* **24,** 6744–6751.
31. Bernhard, W. R., Vašák, M. & Kägi, J. H. R. (1986) *Biochemistry* **25,** 1975–1980.
32. Gan, T., Munoz, A., Shaw, C. F., III & Petering, D. H. (1997) *J. Biol. Chem.* **270,** 5339–5345.
33. Li, H. & Otvos, J. D. (1998) *J. Inorg. Biochem.* **70,** 187–194.
34. Faller, P. & Vašák, M. (1997) *Biochemistry* **36,** 13341–13348.
35. Hasler, D. W., Faller, P. & Vašák, M. (1998) *Biochemistry* **37,** 14966–14973.
36. Faller, P., Hasler, D. W., Zerbe, O., Klauser, S., Winge, D. R. & Vašák, M. (1999) *Biochemistry* **38,** 10158–10167.
37. Cols, N., Romero-Isart, N., Capdevila, M., Oliva, B., Gonzáles-Duarte, P., Gonzáles-Duarte, R. & Atrian, S. (1997) *J. Inorg. Biochem.* **68,** 157–166.